Eighth-order high-temperature expansion for general Heisenberg Hamiltonians

Heinz-Jürgen Schmidt,[1,*] Andre Lohmann,[2] and Johannes Richter[2]
[1]*Universität Osnabrück, Fachbereich Physik, Barbarastr. 7, D-49069 Osnabrück, Germany*
[2]*Institut für Theoretische Physik, Otto-von-Guericke-Universität Magdeburg, PF 4120, D-39016 Magdeburg, Germany*
(Received 20 June 2011; published 26 September 2011)

We explicitly calculate the moments t_n of general Heisenberg Hamiltonians up to eighth order. They have the form of finite sums of products of two factors. The first factor is represented by a (multi-)graph that has to be evaluated for each particular system under consideration. The second factors are well-known universal polynomials in the variable $s(s+1)$, where s denotes the individual spin quantum number. From these moments we determine the corresponding coefficients of the high-temperature expansion of the free energy and the zero field susceptibility by a new method. These coefficients can be written in a form that makes explicit their extensive character. Our results represent a general tool to calculate eighth-order high-temperature series for arbitrary Heisenberg models. The results are applied to concrete systems, namely to magnetic molecules with the geometry of the icosidodecahedron, to frustrated square lattices, and to the pyrochlore magnets. By comparison with other methods that have been recently applied to these systems, we find that the typical susceptibility maximum of the spin-s Heisenberg antiferromagnet is well described by the eighth-order high-temperature series.

DOI: 10.1103/PhysRevB.84.104443 PACS number(s): 75.10.Jm

I. INTRODUCTION

The Heisenberg model

$$H = \sum_{\mu<\nu} J_{\mu\nu} \mathbf{s}_\mu \cdot \mathbf{s}_\nu \tag{1}$$

is the basic model to describe physical properties of magnetic insulators. Despite its simplicity the thermodynamics of the model is generally unknown. For unfrustrated quantum spin systems the quantum Monte Carlo (QMC) method provides accurate numerical results for the temperature dependence of the physical quantities. If the exchange couplings are frustrated the "sign problem" precludes accurate QMC calculations.[1] For one-dimensional (1D) frustrated systems the density-matrix renormalization group approach[2] yields precise results in the whole temperature range. For frustrated quantum spin systems in dimension $D > 1$ accurate methods to calculate thermodynamic properties are notoriously rare. Quite reasonable results for arbitrary temperatures T can be obtained, e.g., by a second-order Green function technique, see, e.g., Refs. 3–5. However, the application of this method needs quite a lot of technical experience. Hence, a simple but universal approach is desirable. A well-established method fulfilling this criterion is the high-temperature expansion (HTE). Since often experimental results, e.g., for the susceptibility, are available in a wide temperature range (including temperatures exceeding the energy scale set by the major exchange constant J, i.e., for $kT \gg |J|$), the HTE can serve as a method to extract the exchange constants of the Heisenberg model from experimental data.

For Heisenberg models on the simple two-dimensional (2D) and three-dimensional (3D) lattices the HTE is available up to high orders; see Refs. 6 and 7 and references therein. However, often one is faced with materials where two or even more different exchange constants are relevant. A typical example are frustrated quasi-1D or quasi-2D magnets where except the nearest-neighbor (NN) and next-nearest-neighbor (NNN) in-chain or in-plane couplings also the interchain or interplane couplings are important. Typically, for such more complex exchange geometries the HTE is known only up to low order. In this situation it would be desirable to have at one's disposal explicit formulas of higher-order HTE for general Heisenberg systems and general spin quantum number s. It is the aim of the present paper to derive such formulas. The key notion is given by the the moments $\mathrm{Tr}\, H^n$ of order n, which can be expressed as sums over suitable sets of graphs. From the moments one can derive the coefficients of the HTE for, say, susceptibility or specific heat in a tedious but straightforward manner. Unfortunately, the number of involved graphs grows super-exponentially with the order n, which delimits the maximal order of the HTE for practical purposes. In this paper, we have confined ourselves to calculations up to eighth order and have to take account of 1139 relevant graphs. Nevertheless, this order is sufficient to describe typical properties of frustrated spin systems, as we will show by means of examples.

The calculation of the HTE for spin systems has a long tradition. Since the 1970s it is known that the moments of certain spin lattices with only one exchange constant can be written as sums over sets of graphs $\mathcal{G}_\nu$ with two factors. The first factor was called the "lattice constant" and counts how often the graph $\mathcal{G}_\nu$ can be embedded into the spin lattice. The second factor is a universal polynomial $p_\nu(r)$ in the variable $r = s(s+1)$. The polynomials $p_\nu(r)$ up to eighth order together with the corresponding graphs $\mathcal{G}_\nu$ are contained in the appendix of Ref. 6. We have independently calculated these polynomials by computer-algebraic means and confirmed a sample of the data in Ref. 6. The generalization of these results from simple spin lattices to arbitrary Heisenberg models is achieved by replacing the above-mentioned "lattice constant" by an "evaluation" of the graph $\mathcal{G}_\nu$ for the spin system under consideration. This evaluation involves sums of products of coupling constants $J_{\mu\nu}$ and yields analytical expressions for the moments of H and the coefficients of the HTE of susceptibility and specific heat. It seems that such general analytical expressions for moments have only be published

up to order three; see Ref. 8. Those papers that consider higher-order expansions, see, e.g., Refs. 9–27, are usually confined to special cases, i.e., special geometries or special values of s. We have used some of these papers, namely Refs. 9, 10, and 26 to check our general results.

The paper is organized as follows. In Sec. II we give the definitions used and illustrate the underlying mathematics. In Sec. III we present general results of the HTE coefficients up to fourth order for the moments of the Hamiltonian, the free energy, and the specific heat, and the magnetic moments and the susceptibility. The very general expressions up to eighth order can be found in Supplemental Material 1.[28] In Sec. IV we apply our method to specific Heisenberg models, which are currently discussed in the literature, namely the Heisenberg antiferromagnet on the Archimedean icosidodecahedron, frustrated square-lattice Heisenberg model, as well as the Heisenberg model on the pyrochlore lattice. For these models the HTE for the specific heat and the susceptibility up to eighth order for arbitrary spin quantum number s are collected in the appendices and Supplemental Material 2.[29]

Although the information provided in this paper and the supplemental materials[28] allows us, in principle, to calculate the HTE up to eighth order, it might be a tedious task to do so in practice. Hence, we provide a simple computer program written in C++ that allows to calculate within a few seconds the eighth-order HTE coefficients as well as the Padé approximants for the susceptibility and the specific heat for an arbitrary Heisenberg model with up to four different exchange constants.[30]

II. DEFINITIONS

In this paper we consider systems of N spins with individual spin quantum number $s = \frac{1}{2}, 1, \frac{3}{2}, \ldots$. The Heisenberg Hamiltonian has the form (1), where the $J_{\mu\nu} = J_{\nu\mu}$, $1 \leqslant \mu \neq \nu \leqslant N$ are suitable coupling constants and $\mathbf{s}_\mu$ denotes the spin vector operator of the μth spin. The moments t_n of H will be normalized by division by the dimension of the total Hilbert space, i.e., $t_n \equiv \frac{\mathrm{Tr}(H^n)}{(2s+1)^N}$. Analogously, the magnetic moments of H are defined by $\mu_n = \frac{\mathrm{Tr}(S^{(3)2} H^n)}{(2s+1)^N}$, where $\mathbf{S}$ denotes the total spin vector and $S^{(i)}$, $i = 1,2,3$, its ith component. As usual, $\chi(\beta) = \beta \frac{\mathrm{Tr}[S^{(3)2} \exp(-\beta H)]}{\mathrm{Tr}[\exp(-\beta H)]}$ denotes the normalized zero field susceptibility. $\chi(\beta) = \sum_{n=1}^{\infty} c_n \beta^n$ is its HTE in terms of the dimensionless inverse temperature $\beta \equiv \frac{|J|}{kT}$, where J is a typical energy. The Hamiltonian H is understood to be dimensionless on division by $|J|$. The free energy $F(\beta)$ is defined by $-\beta F(\beta) = \ln(\mathrm{Tr}\, e^{-\beta H})$ and its HTE is given by $-\beta F(\beta) = \sum_{n=0}^{\infty} a_n \beta^n$. From this one derives the normalized specific heat $C(\beta) \equiv -2\beta^2 \frac{\partial F}{\partial \beta} - \beta^3 \frac{\partial^2 F}{\partial \beta^2}$ and a short calculation shows that its HTE $C(\beta) = \sum_{n=2}^{\infty} d_n \beta^n$ is related to that of $F(\beta)$ by $d_n = n(n-1)a_n$ for $n = 2,3, \ldots$.

HTE are usually written in a compact way by utilizing graph-theoretic notations; see, e.g., Refs. 6 and 7. Let $\mathcal{G}$ be a multigraph consisting of g nodes (vertices) and a number of $\mathcal{N}(i,j) = \mathcal{N}(j,i)$ bonds (edges) between the ith and the jth node. We do not consider "loops," i.e., $\mathcal{N}(i,i) = 0$ for all $i = 1, \ldots, g$. The total number of all bonds, $\gamma(\mathcal{G}) = \sum_{i<j} \mathcal{N}(i,j)$, will be called the size of $\mathcal{G}$. $\mathcal{G}$ is not necessarily connected; see the examples below. We will identify the set of g nodes with $\{1,2,\ldots,g\}$ and the set of N spins with $\{1,2,\ldots,N\}$. To simplify the wording we will omit the prefix "multi-" and simply speak of "graphs" in what follows. A selection of graphs $\mathcal{G}_\nu$, $\nu = 1, \ldots,$ needed for purposes of illustration is represented in Table I. A complete list of all relevant graphs up to size 8 can be found in Supplemental Material 1.[28]

TABLE I. A selection of graphs $\mathcal{G}_\nu$.

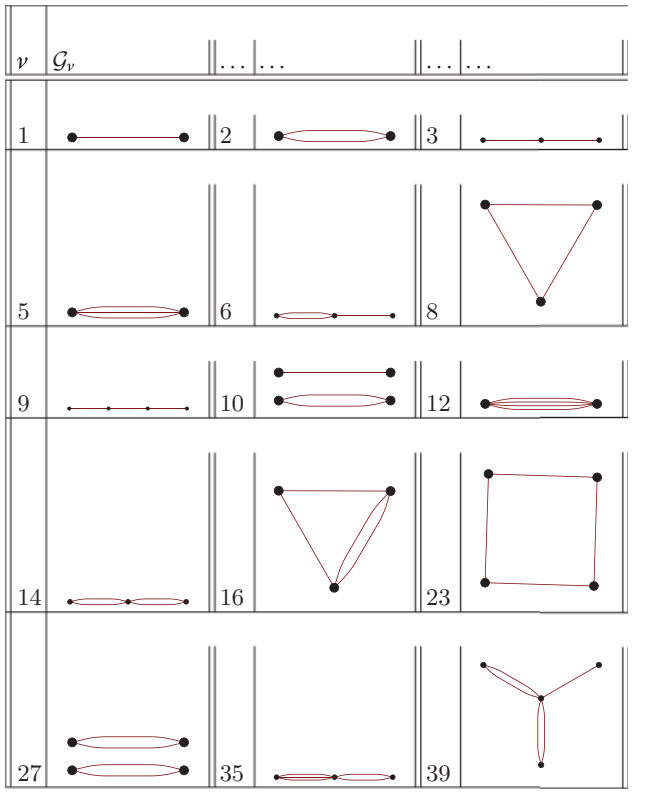

For every graph we define its multinomial factor by

$$f(\mathcal{G}) \equiv \frac{\gamma(\mathcal{G})!}{\prod_{i<j} \mathcal{N}(i,j)!}. \tag{2}$$

Define the symmetry group $G(\mathcal{G})$ of a graph in the obvious way

$$G(\mathcal{G}) \equiv \{\pi \in \mathcal{S}_g | \mathcal{N}(i,j) = \mathcal{N}(\pi(i),\pi(j)) \text{ for all } 1 \leqslant i,j \leqslant g\}. \tag{3}$$

Here $\mathcal{S}_g$ denotes the group of all permutations $\pi : \{1,\ldots,g\} \longrightarrow \{1,\ldots,g\}$. A localization of a graph $\mathcal{G}$ is an embedding

$$\jmath : \{1,\ldots,g\} \longrightarrow \{1,\ldots,N\} \tag{4}$$

up to symmetries of $\mathcal{G}$. More precisely, two embeddings $\jmath_1, \jmath_2 : \{1,\ldots,g\} \longrightarrow \{1,\ldots,N\}$ are called equivalent if and only if $\jmath_1 = \jmath_2 \circ \pi$ for some $\pi \in G(\mathcal{G})$, and a localization of $\mathcal{G}$ is a corresponding equivalence class of embeddings. The number of localizations of $\mathcal{G}$ (for given N) will be denoted by L. We will also speak of localized graphs $\mathcal{G}$ that will be represented by attaching numbers of different spin sites to the nodes of $\mathcal{G}$, with the understanding that two localized graphs that differ only by

a symmetry permutation of the spin sites are considered as identical, e.g.,  .

Two localized graphs $\mathcal{G}_1, \mathcal{G}_2$ can be soldered in a natural way yielding the "soldering product" $\mathcal{G}_1 \oplus \mathcal{G}_2$, which is another localized graph. The nodes of $\mathcal{G}_1 \oplus \mathcal{G}_2$ are identified according to their numbering and the bonds are correspondingly added. For example,

(5)

Conversely, we will say that the localized graph $\mathcal{G}_1 \oplus \mathcal{G}_2$ is decomposed into $\mathcal{G}_1$ and $\mathcal{G}_2$. In general, a localized graph can be decomposed in different ways.

From the expansion

$$\mathrm{Tr} H^n = \sum_{\mu_1 < \nu_1, \ldots, \mu_n < \nu_n} \prod_i J_{\mu_i \nu_i} \ \mathrm{Tr} \left(\prod_i \mathbf{s}_{\mu_i} \cdot \mathbf{s}_{\nu_i} \right) \quad (6)$$

it is clear that the expressions for the moments t_n involve various products of coupling constants $J_{\mu\nu}$. The structure of these products can be represented by the graphs $\mathcal{G}$ defined above, such that the factors $J_{\mu\nu}^{\ell}$ correspond to the bonds of $\mathcal{G}$ with multiplicity ℓ. The sum of different products in (6) of the same structure will be obtained by an evaluation of $\mathcal{G}$, denoted by $\overline{\mathcal{G}}$, for the spin system under consideration. $\overline{\mathcal{G}}$ denotes a real number which depends on the coupling constants and only implicitly on the number N of spins. This number will be defined according to the following statements:

(i) If $g > N$ we set $\overline{\mathcal{G}} = 0$.

(ii) If $g \leqslant N$ we select from each equivalence class of embeddings a certain representative

$$\jmath_\ell : \{1, \ldots, g\} \longrightarrow \{1, \ldots, N\}, \ \ell = 1, \ldots, L \quad (7)$$

and define

$$\overline{\mathcal{G}} \equiv \sum_{\ell=1}^{L} \prod_{1 \leqslant i < j \leqslant g} (J_{\jmath_\ell(i), \jmath_\ell(j)})^{\mathcal{N}(i,j)}. \quad (8)$$

Obviously, the definition of $\overline{\mathcal{G}}$ does not depend on the choice of representatives $\jmath_\ell$ since the product $\prod_{1 \leqslant i < j \leqslant g} (J_{\jmath_\ell(i), \jmath_\ell(j)})^{\mathcal{N}(i,j)}$ is invariant under permutations from the symmetry group $\pi \in G(\mathcal{G})$.

In order to illustrate this definition we consider an example of $N = 4$ spins and $\mathcal{G} = \bigtriangledown$, hence $g = 3 < 4 = N$. The symmetry group $G(\mathcal{G})$ consists of all permutations of {1,2,3}, hence $|G(\mathcal{G})| = 3! = 6$. There are 4! embeddings $\jmath : \{1,2,3\} \longrightarrow \{1,2,3,4\}$ and $L = \frac{4!}{3!} = 4$ equivalence classes from which we choose the representatives

$$\jmath_1 = (1 \to 1, 2 \to 2, 3 \to 3), \quad (9)$$

$$\jmath_2 = (1 \to 1, 2 \to 2, 3 \to 4), \quad (10)$$

$$\jmath_3 = (1 \to 1, 2 \to 3, 3 \to 4), \quad (11)$$

$$\jmath_4 = (1 \to 2, 2 \to 3, 3 \to 4). \quad (12)$$

Hence $\overline{\mathcal{G}} = J_{12}J_{23}J_{13} + J_{23}J_{34}J_{23} + J_{34}J_{14}J_{13} + J_{14}J_{12}J_{24}$.

The coefficients c_n of the susceptibility's HTE (and, similarly, the a_n of the free energy HTE) will contain products of evaluations $\overline{\mathcal{G}_\nu}\ \overline{\mathcal{G}_\mu}$. These expressions can be simplified using rules that transform such products into linear combinations of other evaluations. To give an example, we consider $\overline{\mathcal{G}_1}\ \overline{\mathcal{G}_2} =$ $= (\sum_{\mu<\nu} J_{\mu\nu})(\sum_{\kappa<\lambda} J_{\kappa\lambda}^2)$. It is obvious that this product can be written as a sum over evaluations of the three graphs that can be combined from 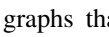 and  , namely , , and . In fact,

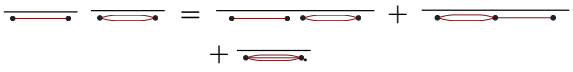

(13)

Similar expressions can be derived for other products of evaluations yielding various "product rules" of the form

$$\overline{\mathcal{G}_\mu}\ \overline{\mathcal{G}_\nu} = \sum_\lambda c_{\mu\nu}^{\lambda}\ \overline{\mathcal{G}_\lambda}. \quad (14)$$

Here the sum over λ runs through all graphs $\mathcal{G}_\lambda$ whose localizations are soldering products of localizations of $\mathcal{G}_\mu$ and $\mathcal{G}_\nu$. The integers $c_{\mu\nu}^{\lambda}$ count the number of ways to decompose a localization of $\mathcal{G}_\lambda$ into localizations of $\mathcal{G}_\mu$ and $\mathcal{G}_\nu$. For example, the decomposition (5) is unique (up to symmetries), hence $c_{2,6}^{35} = 1$; cf. Table I. On the other hand,

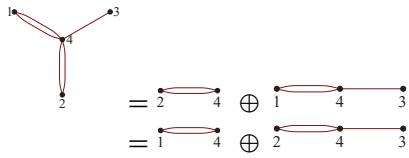

(15)

(16)

hence $c_{2,6}^{39} = 2$; cf. Table I.

In the case $\mathcal{G}_\mu = \mathcal{G}_\nu$ we have to define $c_{\mu\nu}^{\lambda}$ in such a way that the binomial factor 2 is included for products of different localizations. For example,

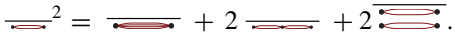

(17)

From the product rules (14) one can derive further ones for multiple products.

III. RESULTS

A. Moments

It turns out that the moments t_n can be written in the following way:

$$t_n = \sum_{\nu \in T_n} \overline{\mathcal{G}_\nu}\ p_\nu(r). \quad (18)$$

Here the $\mathcal{G}_\nu$, $\nu \in T_n$, denote certain graphs of size n and the p_ν are polynomials of order $\leqslant n$ in the variable $r = s(s+1)$. Actually, the p_ν are of the form $p_\nu = \sum_{i=g}^{n} a_i^{(\nu)} r^i$, where g denotes the order of $\mathcal{G}_\nu$ and some $a_i^{(\nu)}$ may vanish. The leading coefficients $a_n^{(\nu)}$ determine the classical limit $r \longrightarrow \infty$ of the moments, hence they can be calculated by means of integrals over unit spheres.

It is crucial that the polynomials p_ν depend neither on N nor on the coupling constants $J_{\mu\nu}$, whereas the terms $\overline{\mathcal{G}_\nu}$ depend only on the coupling constants and only implicitly on N via (8). The polynomials p_ν up to eighth order are well known and have been used for the HTE of certain spin lattices. A subset of the p_ν is, for example, listed in Ref. 6 together with certain rules that permit the calculation of the remaining polynomials.

The most important rule holds in the case where $\mathcal{G}$ is the disjoint union of two simpler graphs, $\mathcal{G} = \mathcal{G}_1 \biguplus \mathcal{G}_2$, and reads

$$p(\mathcal{G}) = p(\mathcal{G}_1)\, p(\mathcal{G}_2) \frac{f(\mathcal{G})}{f(\mathcal{G}_1)\, f(\mathcal{G}_2)}. \tag{19}$$

Note that the polynomials in Ref. 6 are defined as our p_ν divided by the multinomial factor (2), hence these factors do not occur in the rule analogous to (19). Other rules, which we need not repeat here, say that the p_ν vanish *a priori* for certain graphs.

For the determination of t_n it thus suffices to enumerate the graphs $\mathcal{G}_\nu$, $\nu \in T_n$ and the corresponding polynomials p_ν. We will give the first four moments for the sake of illustration and defer the lengthy expressions for $t_n, n = 5,6,7,8$ to the Supplemental Material 1.[28]

$$t_1 = 0 \tag{20}$$

$$t_2 = \sum_{\mu<\nu} J_{\mu\nu}^2 \, \frac{1}{3} r^2 = \frac{1}{3} r^2 \, \overline{\mathcal{G}_2}, \tag{21}$$

$$t_3 = -\frac{1}{6} r^2 \, \overline{\mathcal{G}_5} + \frac{2}{3} r^3 \, \overline{\mathcal{G}_8}, \tag{22}$$

$$t_4 = \frac{1}{15} r^2 (2 - 2r + 3r^2) \, \overline{\mathcal{G}_{12}} + \frac{2}{9} r^3 (-1 + 3r) \, \overline{\mathcal{G}_{14}} - \frac{2}{9} r^3 \, \overline{\mathcal{G}_{16}} + \frac{8}{9} r^4 \, \overline{\mathcal{G}_{23}} + \frac{2}{3} r^4 \, \overline{\mathcal{G}_{27}}. \tag{23}$$

B. Free energy

It is well known that the coefficients of the power series for the free energy $F(\beta)$

$$-\beta F(\beta) = \ln(\mathrm{Tr}\, e^{-\beta H}) = \sum_{n=0}^{\infty} a_n \beta^n \tag{24}$$

can be expressed in terms of the moments t_n and its products. As indicated in Sec. II, a variety of product rules can be used to simplify the resulting expressions. This simplification, which is sometimes also referred to as the "cumulant expansion," see, e.g., Ref. 7, has the further advantage that it reveals the extensive character of the a_n. By this we mean the following. If the spin system under consideration would have a periodic lattice structure of, say, K unit cells with periodic boundary conditions, it follows immediately that the evaluation of a single graph $\overline{\mathcal{G}}$ linearly scales with K, and hence with N, as long as $\mathcal{G}$ is connected. For unconnected $\mathcal{G}$ the evaluation scales with K^c, where c is the number of connected components of $\mathcal{G}$. Obviously, products of evaluations of connected graphs $\overline{\mathcal{G}_\nu}\, \overline{\mathcal{G}_\mu}$ would scale with K^2. It turns out that the elimination of these and higher products in the expression for the a_n by means of the rules (14) also eliminates the evaluation terms of unconnected graphs. This has to be expected on physical grounds, since the total free energy of a spin lattice should be an extensive quantity, i.e., linearly scale with K. But it is an additional consistency test of our results that the nonextensive contributions to the a_n actually cancel.

The first five coefficients of the series (24) read as follows:

$$a_0 = N \, \ln(2s+1), \tag{25}$$

$$a_1 = 0, \tag{26}$$

$$a_2 = \frac{1}{6} r^2 \, \overline{\mathcal{G}_2}, \tag{27}$$

$$a_3 = \frac{1}{36} r^2 \, \overline{\mathcal{G}_5} - \frac{1}{9} r^3 \, \overline{\mathcal{G}_8}, \tag{28}$$

$$a_4 = -\frac{1}{180} r^2 (-1 + r + r^2) \, \overline{\mathcal{G}_{12}} - \frac{1}{108} r^3 \, \overline{\mathcal{G}_{14}} - \frac{1}{108} r^3 \, \overline{\mathcal{G}_{16}} + \frac{1}{27} r^4 \, \overline{\mathcal{G}_{23}}. \tag{29}$$

The a_n, $n = 5,6,7,8$ are given in Supplemental Material 1.[28]

C. Magnetic moments and susceptibility

To obtain the magnetic moments μ_n we will adopt a special method that is available if one knows the moments t_n for all values of the coupling constants $J_{\mu\nu}$. We replace H by the one parameter family of Hamiltonians $H_\alpha \equiv H + \frac{\alpha}{2}(\mathbf{S}^2 - Nr)$. Equivalently, we can substitute $J_{\mu\nu} \mapsto J_{\mu\nu} + \alpha$ for all coupling constants. The magnetic moments then result from differentiating $\mathrm{Tr}(H_\alpha^{n+1})$ with respect to α and, finally, setting $\alpha = 0$:

$$\frac{\partial}{\partial \alpha} \mathrm{Tr}\big(H_\alpha^{n+1}\big)\Big|_{\alpha=0} = \frac{n+1}{2} \mathrm{Tr}\big[H_0^n (\mathbf{S}^2 - Nr)\big] = \frac{(n+1)(2s+1)^N}{2} (3\mu_n - Nr t_n). \tag{30}$$

We can calculate the left-hand side of (30) if we insert the results for the moments and consider "derivatives" $\mathcal{G}'$ of graphs defined in the following way. Let $\mathcal{G}^{(ij)}$ denote the graph $\mathcal{G}$ but with one bond removed, $\mathcal{N}(i,j) \mapsto \mathcal{N}(i,j) - 1$. If $\mathcal{N}(i,j) = 0$ then we set $\mathcal{G}^{(ij)} = 0$. Further let $G(\mathcal{G})$ and $G(\mathcal{G}^{(ij)})$ denote the respective symmetry groups. Then we define

$$\mathcal{G}' = \sum_{i<j} \mathcal{N}(i,j) \, \mathcal{G}^{(ij)} \, \frac{|G(\mathcal{G}^{(ij)})|}{|G(\mathcal{G})|}. \tag{31}$$

One has, so to speak, to break each bond of the graph and to sum over all results. Further, one has to introduce factors that compensate for the possible change of symmetries. For example $\mathcal{G}'_{16} = 6\mathcal{G}_8 + \mathcal{G}_6$, see Table I. It is obvious that the evaluation of $\mathcal{G}'$ just yields $\frac{\partial}{\partial \alpha} \overline{\mathcal{G}}|_{\alpha=0}$. Then it is a straightforward task to calculate the magnetic moments $\mu_0, \ldots, \mu_7$ by using the above results for the t_n. We will display the results for $\mu_n, n = 0,1,2,3$ and give the remaining $\mu_n, n = 4,5,6,7$ in Supplemental Material 1.[28]

$$\mu_0 = \frac{Nr}{3}, \tag{32}$$

$$\mu_1 = \frac{2}{9} r^2 \, \overline{\mathcal{G}_1}, \tag{33}$$

$$\mu_2 = \frac{1}{9} r^2 (Nr - 1) \, \overline{\mathcal{G}_2} + \frac{4}{27} r^3 \, \overline{\mathcal{G}_3}, \tag{34}$$

$$\mu_3 = \frac{1}{90} r^2 (8 - (8 + 5N) r + 12 r^2) \, \overline{\mathcal{G}_5} + \frac{1}{9} r^3 (-1 + 2r) \, \overline{\mathcal{G}_6} + \frac{2}{9} r^3 (-1 + Nr) \, \overline{\mathcal{G}_8} + \frac{4}{27} r^4 \, \overline{\mathcal{G}_9} + \frac{2}{9} r^4 \, \overline{\mathcal{G}_{10}}. \tag{35}$$

The coefficients of the high temperature expansion of $\chi = \beta \frac{\mathrm{Tr}[S^{(3)2} \exp(-\beta H)]}{\mathrm{Tr}[\exp(-\beta H)]}$ can be expressed through the μ_n and the t_n

that occur as coefficients of the series in the numerator or in the denominator, respectively. The first four coefficients are given by

$$\chi = \sum_{n=1}^{\infty} c_n\, \beta^n = \mu_0\, \beta - \mu_1\, \beta^2 + \frac{1}{2}(\mu_2 - \mu_0\, t_2)\beta^3 + \frac{1}{6}(t_3\mu_0 + 3t_2\mu_1 - \mu_3)\beta^4 + \ldots. \tag{36}$$

Inserting the known values for t_n and μ_n yields the desired results for c_n. Similarly as in Sec. III B, a variety of product rules can be used to simplify the resulting expressions revealing the extensive character of c_n.

We will represent the results for the susceptibility's HTE up to fourth order in the inverse temperature β. The higher coefficients $c_n, n = 5,6,7,8$ will be given in Supplemental Material 1:[28]

$$c_1 = \frac{Nr}{3}, \tag{37}$$

$$c_2 = -\frac{2}{9}r^2\,\overline{\mathcal{G}_1}, \tag{38}$$

$$c_3 = -\frac{1}{18}r^2\,\overline{\mathcal{G}_2} + \frac{2}{27}r^3\,\overline{\mathcal{G}_3}, \tag{39}$$

$$c_4 = \frac{2}{135}r^2(-1 + r + r^2)\,\overline{\mathcal{G}_5} + \frac{1}{54}r^3\,\overline{\mathcal{G}_6} + \frac{1}{27}r^3\,\overline{\mathcal{G}_8} - \frac{2}{81}r^4\,\overline{\mathcal{G}_9}. \tag{40}$$

IV. APPLICATION TO FRUSTRATED HEISENBERG SYSTEMS

To improve the HTE approximation, G. A. Baker has introduced Padé approximants[31] (see also Refs. 6 and 7). These ratios of two polynomials $[m,n] = P_m(x)/R_n(x)$ of degree m and n provide an analytic continuation of a function $f(x)$ given by a power series, and, therefore, they yield a better approximation of the function $f(x)$. As a rule, approximants with $m = n$ provide best results. Since we have a power series up to eighth order, we use the corresponding [4,4] Padé approximant.

A. The Keplerate magnetic molecules

In the Keplerate molecules $Mo_{72}Fe_{30}$, $Mo_{72}Cr_{30}$, $Mo_{72}V_{30}$, and $W_{72}V_{30}$ the magnetic ions sit on the vertices of an almost perfect icosidodecahedron[32–35]; see Fig. 1. Moreover, the interactions between the magnetic ions are well described by the Heisenberg model (1) with NN interactions. These molecules have attracted much attention from the experiment[32–37] and theory.[36–43] One reason is that their frustrated exchange geometry has much in common with the kagome lattice; see, e.g., Refs. 44 and 45. For the $Mo_{72}V_{30}$ and $W_{72}V_{30}$ molecules the spin quantum number is $s = 1/2$, which allows us to calculate low-energy states exactly by Lanczos exact diagonalization.[38] For spin quantum numbers $s > 1/2$ that is already impossible, i.e., for $Mo_{72}Cr_{30}$ ($s = 3/2$) and $Mo_{72}Fe_{30}$ ($s = 5/2$) the low-energy spectrum can be found only approximately.[36,39] To evaluate thermodynamic properties already for $s = 1/2$ one has to use approximations.[42,43] Only at high magnetic fields and low temperatures numerical exact results were reported.[41] Very recently a finite-temperature Lanczos approximation has been used[43] to describe the magnetic properties of $W_{72}V_{30}$ at finite temperatures, and it has been found that the theoretical results agree well with the experimental data over a wide temperature range. However, for frustrated quantum spin systems with $s > 1/2$ the calculation of thermodynamic quantities is even more challenging. Hence our HTE seems to be useful, in particular, for $s > 1/2$. The HTE series for the susceptibility and the specific heat for arbitrary spin quantum number are given in Eqs. (A1) and (A2) in Appendix A.

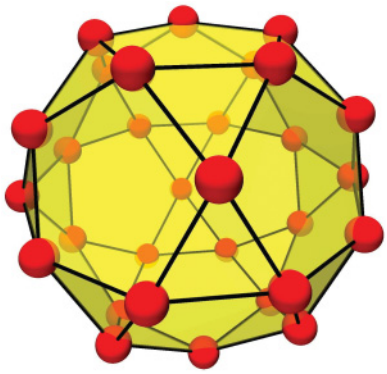

FIG. 1. (Color online) The Archimedean solid icosidodecahedron. In the magnetic molecules $Mo_{72}Fe_{30}$, $Mo_{72}Cr_{30}$, $Mo_{72}V_{30}$, and $W_{72}V_{30}$ the magnetic ions occupy the vertices (red bullets).

We focus on the analysis of the HTE data for the susceptibility, since the high temperature magnetic part of the specific heat often cannot be accurately separated from the phonon part. First we compare our $s = 1/2$ HTE result for χ with experimental[35] and theoretical[43] data for $W_{72}V_{30}$. In Fig. 2 we show the $T\chi$ vs. T curve as done in Refs. 43 and 35. While

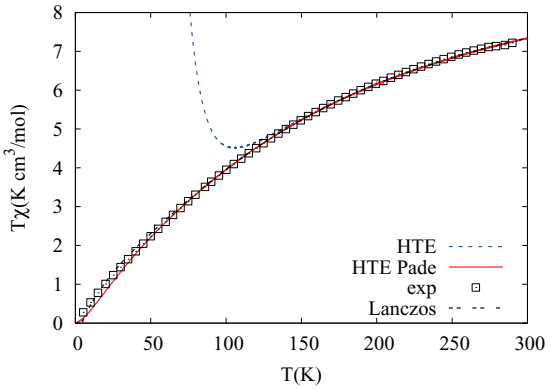

FIG. 2. (Color online) Susceptibility times temperature in dependence on the temperature. The symbols show the experimental data for $Mo_{72}Cr_{30}$ (Ref. 35), the black dashed line represents the finite-temperature Lanczos result,[43] the blue dashed line shows the pure HTE results, and the red solid line the [4,4] Padé approximant of the HTE series. For the exchange parameter J and the spectroscopic splitting factor g we have used the same values as in Refs. 35 and 43, namely $J/k = 115$ K and $g = 1.95$. Note that the Padé approximant and the finite-temperature Lanczos data in a wide temperature range practically coincide.

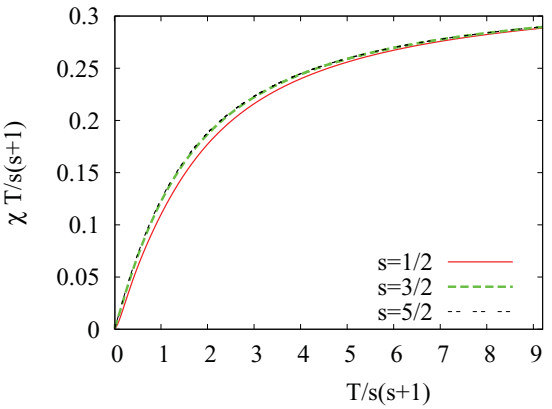

FIG. 3. (Color online) Results of the HTE-Padé approximant for the susceptibility times temperature in dependence on the temperature (arbitrary units) for spin quantum numbers $s = 1/2$, $s = 3/2$, and $s = 5/2$.

the raw HTE data start to deviate from the experimental ones at about $T = 115$K we find an excellent agreement with the experimental results and the previous theoretical simulations if we use the [4,4] Padé approximant.

Next we compare in Fig. 3 our results for χ for the spin quantum numbers $s = 1/2$, $3/2$, $5/2$ relevant for $Mo_{72}V_{30}$, $W_{72}V_{30}$, $Mo_{72}Cr_{30}$, and $Mo_{72}Fe_{30}$. Again we show $T\chi$ vs. T, since such a plot is used in many experimental papers; see, e.g., Refs. 35, 34, and 44. Suggested by Eq. (A1) given in Appendix A we use a renormalized temperature $T/s(s+1)$, i.e., we show the dependence $T\chi/s(s+1)$ vs. $T/s(s+1)$ in Fig. 3. Obviously, the curves for different s are very close to each other. From Eq. (A1) it is obvious that with increasing spin quantum number s in each order of $\beta = 1/kT$ the highest order in $r = s(s+1)$ yields the dominant contribution, and therefore the plot $T\chi/s(s+1)$ vs. $T/s(s+1)$ becomes independent of s for larger values of s. However, from both Figs. 2 and 3 the question arises whether the $T\chi/s(s+1)$ vs. $T/s(s+1)$ plot

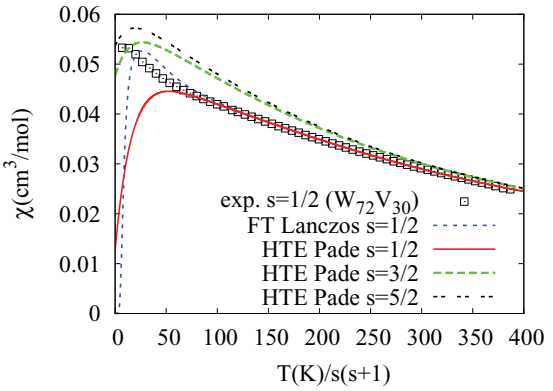

FIG. 4. (Color online) Results of the HTE-Padé approximant for the susceptibility in dependence on the temperature for the Keplerate magnetic molecule for spin quantum numbers $s = 1/2$, $s = 3/2$, $s = 5/2$ compared with experimental data for the $s = 1/2$ system $W_{72}V_{30}$[35] (symbols) and finite-temperature Lanczos results for $s = 1/2$[43] (blue dashed line). For the exchange parameter J and the spectroscopic splitting factor g we have used the same values as in Refs. 35 and 43, namely $J/k = 115$ K and $g = 1.95$.

is appropriate to detect specific features in χ, in particular at low temperatures. Indeed, the plots in Fig. 4 demonstrate that the characteristic low-temperature maximum in χ is masked in the $T\chi/s(s+1)$ vs. $T/s(s+1)$ plot. The height and the position of the maximum in χ clearly depend on s. From Fig. 4 it is obvious that its position is shifted to lower values of $T/s(s+1)$ while its height is increasing with growing s.

B. The square-lattice J_1-J_1'-J_2-J_2' model

Next we consider spin systems on infinite lattices. As an example, we focus on the frequently discussed square-lattice Heisenberg magnet with NN couplings J_1 and frustrating NNN bonds J_2, the so-called J_1-J_2 model. This system has attracted a great deal of interest as a model system to study quantum phase transitions; see, e.g., the recent publications[46–52] and references therein. The HTE for the spin-$1/2$ J_1-J_2 model was presented in Ref. 26.

The interest in this model is also promoted by a number of experimental investigations on magnetic materials described reasonably well by the J_1-J_2 model. However, in real materials, one is often faced with deviations from the ideal J_1-J_2 model. For instance, in layered vanadium phosphates[53,54] due to low crystal symmetry the bonds along the sides and the diagonals of the square can be nonequivalent. Hence, in a realistic spin model for these compounds one has to consider two independent NN and two independent NNN exchange parameters. Therefore, we consider here a generalized J_1-J_1'-J_2-J_2' model

$$H = \sum_{\nu} (J_1 \mathbf{s}_\nu \cdot \mathbf{s}_{\nu+x} + J_1' \mathbf{s}_\nu \cdot \mathbf{s}_{\nu+y} + J_2 \mathbf{s}_\nu \cdot \mathbf{s}_{\nu+x+y} + J_2' \mathbf{s}_\nu \cdot \mathbf{s}_{\nu+x-y}), \quad (41)$$

which is more appropriate to provide a realistic description of frustrated square-lattice materials such as the layered vanadium phosphates. The exchange pattern of the model (41) is illustrated in Fig. 5.

Based on our general formulas we get the coefficients of the high-temperature expansion for the susceptibility and the specific heat for the generalized model (41); see Appendix B and Supplemental Material 2.[29] These formulas also contain interesting limits of coupled chain systems[55–58] obtained by an appropriate choice of the coupling constants.

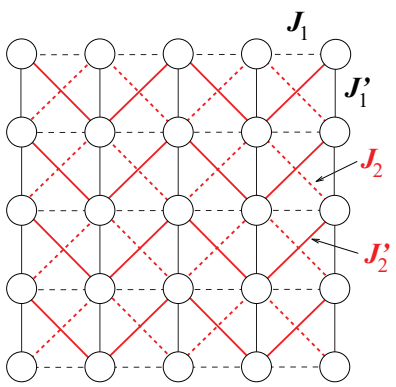

FIG. 5. (Color online) Illustration of the exchange paths for the anisotropic frustrated square-lattice model (41).

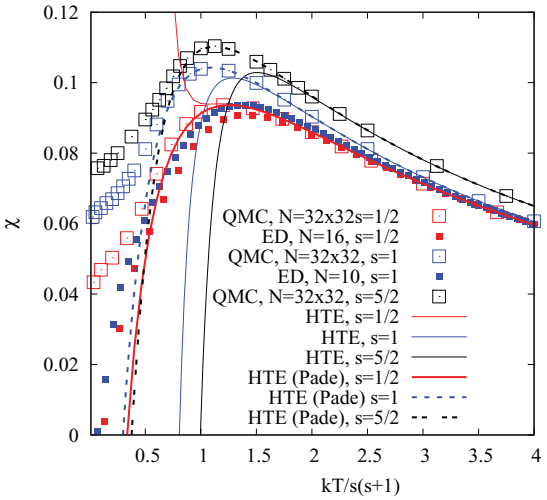

FIG. 6. (Color online) Susceptibility χ of the unfrustrated Heisenberg antiferromagnet [i.e., $J_1' = J_1 = 1$, $J_2' = J_2 = 0$ in Eq. (41)] for spin quantum numbers $s = 1/2, s = 1$, and $s = 5/2$. The data of the pure HTE series and the Padé approximant are compared with corresponding QMC (taken from Ref. 52) and ED results.

First, we compare in Fig. 6 the HTE data for the susceptibility with accurate QMC data for the pure square lattice Heisenberg antiferromagnet for $s = 1/2$, $s = 1$, and $s = 5/2$; see, e.g., Refs. 59, 60, and 52, as well as with numerical exact data for finite lattices obtained by full exact diagonalization (ED). Again, we use the renormalized temperature $T/s(s+1)$ for the plot; see the discussion in the previous section. The comparison with precise QMC data allows to estimate that temperature T_a down to which the HTE approximation for χ is accurate. We find that the pure HTE in eighth order practically coincides with QMC data until $T_{a,1}/[J_1 s(s+1)] = 1.2$, 1.4, and 2.0 for $s = 1/2$, $s = 1$, and $s = 5/2$, respectively. Using the [4,4] Padé approximant we find $T_{a,2}/[J_1 s(s+1)] = 0.85$, 0.75, and 0.95 for $s = 1/2$, $s = 1$, and $s = 5/2$, respectively, and it is evident from Fig. 6 that the maximum in χ is described accurately. Even significantly below $T_{a,2}$ the Padé approximant describes the QMC data reasonably well. Moreover, by comparison with ED data we can figure out how good typical ED results can describe realistic large systems in two dimensions. Often, the ED is used as the only method to discuss the thermodynamics of strongly frustrated 2D quantum spin systems; see, e.g., Refs. 53 and 61–63. The results shown in Fig. 6 indicate that for 2D systems already at moderate temperatures and even for $s = 1/2$ (where largest systems are accessible by ED) significant finite-size effects appear and that our HTE results for $N \to \infty$ are better than typical ED results. A similar finding was reported in Ref. 5 where ED results for χ are compared with data of a Green's function approach for a spin-1/2 frustrated square-lattice ferromagnet.

We consider now the generalized J_1-J_1'-J_2-J_2' model (41) relevant for layered vanadium phosphates.[53,54] First, we mention that, for the symmetric model (i.e., $J_1 = J_1'$, $J_2 = J_2'$), we give the general formulas for the HTE coefficients for arbitrary s up to eighth order in Appendix B. For the asymmetric model for arbitrary s the formulas become very lengthy for higher orders. Therefore, in Appendix B we present the formulas for arbitrary s only up to fifth order and give the remaining sixth to eighth orders in Supplemental Material 2.[29] To illustrate our HTE results we follow the lines of Ref. 53 and discuss the influence of exchange asymmetry $J_1 \neq J_1'$, $J_2 \neq J_2'$ on the temperature dependence of the susceptibility, in particular, on the position and the height of the maximum in χ. This issue was discussed Ref. 53 based on ED data for $N = 16 = 4 \times 4$ (see Fig. 9 therein). We have repeated these ED calculation and compare the ED results with the HTE data for $N = 16$ and $N \to \infty$ in Fig. 7 and in Table II.

Obviously for $N = 16$ the ED and the corresponding HTE-Padé data for the maximum in χ agree well. But it is also obvious, that the finite-size data for the maximum do not agree well with data for $N \to \infty$. The shift of the maximum by varying the asymmetry (i.e., the difference in J_1 and J_1' or/and in J_2 and J_2') discussed Ref. 53 is not observed (or is at least much less pronounced) in the HTE results for $N \to \infty$; cf. Fig. 7 and Table II. Hence we argue again that the conclusions based on finite-temperature ED data for 2D systems might be not reliable for large systems.

C. The Heisenberg model on the pyrochlore lattice

As the last example we consider a 3D frustrated spin system, namely the Heisenberg model on the pyrochlore lattice. In three dimensions the ED is not applicable to calculate

TABLE II. Position $T_m = T_{\max}/J_c$ and height $\chi_m = \chi_{\max} J_c/(N_A g^2 \mu_B^2)$ of the susceptibility maximum of the model (41). In the table we compare the numerical exact ED data for $N = 16$ (superscript ED), the corresponding HTE-Padé data for $N = 16$ (superscript HTE_{16}) and the HTE-Padé data for $N = \infty$ (superscript HTE_∞). The thermodynamic energy scale is defined as $J_c = \sqrt{(J_1^2 + J_1'^2 + J_2^2 + J_2'^2)/2}$.

J_1	J_1'	J_2	J_2'	T_m^{ED}	χ_m^{ED}	$T_m^{\mathrm{HTE}_{16}}$	$\chi_m^{\mathrm{HTE}_{16}}$	$T_m^{\mathrm{HTE}_\infty}$	$\chi_m^{\mathrm{HTE}_\infty}$
$-\frac{1}{2}$	$-\frac{1}{2}$	2	0	1.02	0.1214	1.02	0.1214	0.83	0.1290
$-\frac{1}{2}$	$-\frac{1}{2}$	$\frac{8}{5}$	$\frac{2}{5}$	0.99	0.1199	1.01	0.1197	0.81	0.1284
$-\frac{1}{2}$	$-\frac{1}{2}$	$\frac{4}{3}$	$\frac{2}{3}$	1.00	0.1181	1.04	0.1174	0.80	0.1287
$-\frac{1}{2}$	$-\frac{1}{2}$	$\frac{8}{7}$	$\frac{6}{7}$	1.02	0.1170	1.06	0.1159	0.80	0.1291
$-\frac{1}{2}$	$-\frac{1}{2}$	1	1	1.02	0.1167	1.07	0.1155	0.80	0.1291
$-\frac{4}{7}$	$-\frac{3}{7}$	1	1	1.03	0.1165	1.08	0.1152	0.80	0.1288
$-\frac{2}{3}$	$-\frac{1}{3}$	1	1	1.05	0.1154	1.11	0.1141	0.83	0.1276
$-\frac{4}{5}$	$-\frac{1}{5}$	1	1	1.10	0.1136	1.17	0.1118	0.89	0.1254
-1	0	1	1	1.15	0.1115	1.22	0.1097	0.96	0.1225

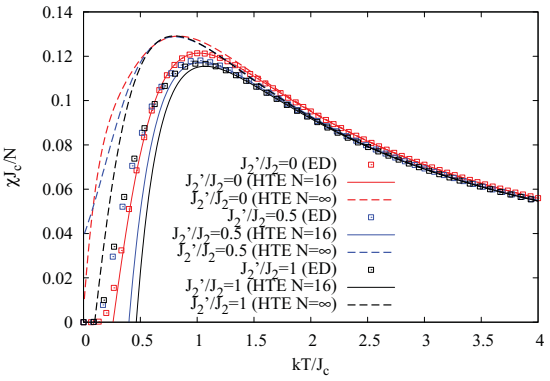

FIG. 7. (Color online) Comparison of ED and HTE-Padé results for the susceptibility of the frustrated model (41) for spin quantum number $s = 1/2$. For the exchange parameters we follow Ref. 53 and choose $J_1 = J_1' = -1/2$ and $(J_2 + J_2')/(J_1 + J_1') = -2$. The thermodynamic energy scale is defined as $J_c = \sqrt{(J_1^2 + J_1'^2 + J_2^2 + J_2'^2)/2}$.

reasonably well thermodynamic properties. Moreover, typically there is finite-temperature phase transition that needs special analysis of the HTE series. The pyrochlore lattice is highly frustrated and it has attracted much attention over the past few years; see, e.g., Refs. 64–66 and references therein. To the best of our knowledge so far no higher-order HTE has been presented. For the classical limit the thermodynamics was investigated systematically mainly by classical Monte Carlo (MC) simulations; see, e.g., Refs. 67, 68, and 69. Due to strong frustration there is no phase transition to an ordered low-temperature phase for the pyrochlore Heisenberg antiferromagnet. For the quantum model no precise data are available at lower temperatures.

The HTE series for the susceptibility and the specific heat for arbitrary spin quantum number s are given in Eqs. (C1) and (C2) in Appendix C. The plots of the Padé approximants for the Heisenberg antiferromagnet are shown in Fig. 8 for various

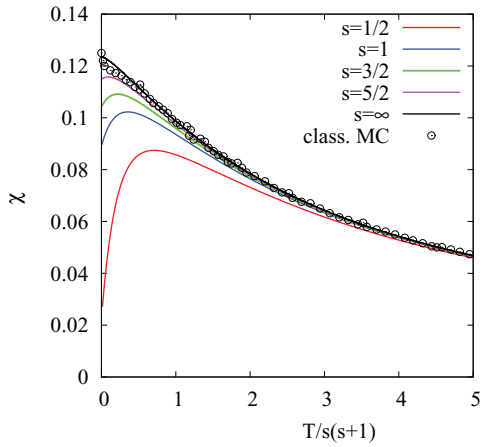

FIG. 8. (Color online) HTE Padé approximant for the susceptibility of pyrochlore Heisenberg antiferromagnet for $s = 1/2$, 1, 3/2, 5/2, and $s \to \infty$. The MC data for $s \to \infty$ are taken from Refs. 68 and 69.

values of s. For the classical model ($s \to \infty$) we compare our HTE data with MC data calculated in Ref. 68; see also Ref. 69. Surprisingly, there is excellent agreement with the MC data down to temperatures that are considerably below $|J|/k$. In particular, the fact that there is no maximum in the $\chi(T)$ curve is observed both in MC and HTE results. Lowering the quantum number s, i.e., increasing the quantum fluctuations a low-temperature maximum in $\chi(T)$ emerges. The height χ_m of the maximum decreases, whereas the position $T_m/s(s+1)$ increases with decreasing of s.

V. CONCLUSIONS

In this paper we provide general expressions for the high-temperature expansion series up to the eighth order of free energy, the specific heat, and the susceptibility for Heisenberg models with arbitrary exchange patterns $J_{\mu\nu}$ and spin quantum number s. These formulas can be used as a tool to investigate thermodynamic properties of general Heisenberg systems and thus for the interpretation of experimental data, especially if other precise methods, such as the quantum Monte Carlo method or the finite-temperature density matrix renormalization group approach, are not applicable. By comparison with precise quantum Monte Carlo results for the susceptibility χ of the unfrustrated 2D Heisenberg antiferromagnet with NN exchange J with $s = 1/2$, $s = 1, \ldots$, $s = 5/2$ we find that the HTE results yield the correct susceptibility at high temperatures down up to $T/s(s+1) \approx |J|/k$. Using Padé approximants the accuracy can be extended to lower temperatures. In particular, the typical maximum in χ for the Heisenberg antiferromagnet can be well described using the HTE of eighth order.

We apply our method to frustrated systems, namely to frustrated Keplerate magnetic molecules, to a frustrated square-lattice Heisenberg magnet, and to a pyrochlore Heisenberg magnet. By comparison with finite-size data for the unfrustrated as well as the frustrated square-lattice Heisenberg model obtained by full exact diagonalization we find that the size of 2D systems accessible by full exact diagonalization seems to be too small to get precise data for the susceptibility maximum. The comparison with Monte Carlo data for the classical pyrochlore Heisenberg antiferromagnet yields excellent agreement down to low temperatures.

ACKNOWLEDGMENT

We thank J. Schnack for providing the data from Ref. 43 used in Fig. 2. For the exact diagonalization J. Schulenburg's *spinpack* was used.

APPENDIX A: THE HIGH-TEMPERATURE EXPANSION FOR THE SUSCEPTIBILITY AND THE SPECIFIC HEAT FOR THE HEISENBERG MODEL ON THE ICOSIDODECAHEDRON WITH NEAREST-NEIGHBOR EXCHANGE INTERACTION

The general formulas for the susceptibility and the specific heat for the Heisenberg model on the icosidodecahedron with the NN exchange constant J up to eighth order

read

$$\chi(\beta) = \frac{N}{J}\sum_{n=1}^{\infty} c_n (J\beta)^n;\ r = s(s+1)$$
$$c_1 = \frac{1}{3}\,r;\ \ c_2 = -\frac{4}{9}\,r^2;\ \ c_3 = \frac{1}{9}\,r^2(4\,r-1);\ \ c_4 = -\frac{4}{405}\,r^2(3-28\,r+37\,r^2)$$
$$c_5 = \frac{r^2}{4860}(-45+702\,r-1892\,r^2+1328\,r^3)$$
$$c_6 = -\frac{r^2}{510\,300}(1728-35\,946\,r+164\,289\,r^2-209\,296\,r^3+99\,776\,r^4) \tag{A1}$$
$$c_7 = \frac{r^2}{2\,041\,200}(-2898+72\,972\,r-467\,127\,r^2+967\,124\,r^3-765\,536\,r^4+259\,008\,r^5)$$
$$c_8 = -\frac{r^2}{11\,481\,750}(7695-223\,128\,r+1\,769\,382\,r^2-5\,284\,101\,r^3+6\,231\,056\,r^4-3\,632\,860\,r^5+745\,760\,r^6)$$

and

$$C(\beta) = Nk\sum_{n=2}^{\infty} d_n (J\beta)^n$$
$$d_2 = \frac{2}{3}\,r^2;\ \ d_3 = \frac{r^2}{9}(3-4\,r);\ \ d_4 = -\frac{2}{45}\,r^2(-3+23\,r+3\,r^2)$$
$$d_5 = \frac{r^2}{162}(9-126\,r+116\,r^2+32\,r^3)$$
$$d_6 = \frac{r^2}{22\,680}(576-11\,142\,r+34\,323\,r^2+5088\,r^3+3952\,r^4) \tag{A2}$$
$$d_7 = -\frac{r^2}{97\,200}(-1242+29\,556\,r-150\,039\,r^2+100\,736\,r^3+32\,624\,r^4+25\,472\,r^5)$$
$$d_8 = -\frac{r^2}{1\,093\,500}(-7695+213\,084\,r-1\,435\,806\,r^2+2\,566\,548\,r^3+214\,682\,r^4+473\,600\,r^5+82\,120\,r^6).$$

APPENDIX B: THE HIGH-TEMPERATURE EXPANSION FOR THE SUSCEPTIBILITY AND THE SPECIFIC HEAT FOR THE SQUARE-LATTICE J_1-J_1'-J_2-J_2' MODEL

Here we list the general formulas for the susceptibility and the specific heat for the J_1-J_1'-J_2-J_2' model defined in Eq. (41). Since the corresponding formulas become very lengthy in higher orders of the HTE, we restrict ourselves here to (i) general formulas for the symmetric model ($J_1 = J_1'$ and $J_2 = J_2'$) for arbitrary spin quantum number s up to eighth order and (ii) general formulas for the asymmetric model ($J_1 \neq J_1'$ and $J_2 \neq J_2'$) for arbitrary s up to fifth order, only (for the remaining sixth- to eighth-order coefficients, see Supplemental Material 2[29]). Note that for the symmetric models with $s = 1/2$ the HTE coefficients up to 10th order are given in Ref. 26.

First we give the formulas for the symmetric model:

$$\chi(\beta) = N\sum_{n=1}^{\infty} c_n \beta^n;\ r = s(s+1)$$
$$c_1 = \frac{r}{3};\quad c_2 = -\frac{4}{9}r^2(J_1+J_2);\quad c_3 = \frac{1}{27}r^2\left[3J_1^2(-1+4r)+32J_1J_2r+3J_2^2(-1+4r)\right]$$
$$c_4 = -\frac{2}{405}r^2\left[3J_1^3(2-17r+28r^2)+10J_1^2J_2r(-9+34r)+20J_1J_2^2r(-3+20r)+3J_2^3(2-17r+28r^2)\right]$$
$$c_5 = \frac{1}{4860}r^2\left[J_1^4(-45+648r-1808r^2+1712r^3)+120J_1^3J_2r(5-54r+80r^2)+12J_1^2J_2^2r(69-574r+1536r^2)\right.$$
$$\left.+192J_1J_2^3r(2-27r+68r^2)+J_2^4(-45+648r-1808r^2+1712r^3)\right]$$

$$
\begin{aligned}
c_6 = &-\frac{1}{127\,575}r^2\big[2J_1^5(216-4131r+18\,339r^2-28\,710r^3+18\,100r^4)+21J_1^4J_2r(-279+4801r-14\,048r^2+12\,368r^3)\\
&+14J_1^3J_2^2r(-477+7158r-40\,044r^2+49\,864r^3)+35J_1^2J_2^3r(-216+3261r-13\,504r^2+24\,240r^3)\\
&+350J_1J_2^4r(-9+186r-832r^2+1168r^3)+2J_2^5(216-4131r+18\,339r^2-28\,710r^3+18\,100r^4)\big]\\
c_7 = &\frac{1}{3\,061\,800}r^2\big[J_1^6(-4347+99\,738r-623\,943r^2+1\,392\,666r^3-1\,440\,944r^4+673\,152r^5)\\
&+28J_1^5J_2r(2133-44\,406r+223\,896r^2-351\,328r^3+209\,664r^4)\\
&+42J_1^4J_2^2r(1620-35\,649r+248\,050r^2-618\,992r^3+485\,984r^4)\\
&+28J_1^3J_2^3r(2061-46\,134r+389\,520r^2-1\,234\,240r^3+1\,254\,912r^4)\\
&+2J_1^2J_2^4r(36\,936-789\,687r+4\,517\,328r^2-12\,128\,272r^3+15\,232\,512r^4)\\
&+64J_1J_2^5r(432-11\,097r+75\,108r^2-181\,180r^3+166\,680r^4)\\
&+J_2^6(-4347+99\,738r-623\,943r^2+1\,392\,666r^3-1\,440\,944r^4+673\,152r^5)\big]\\
c_8 = &-\frac{1}{91\,854\,000}r^2\big[3J_1^7(20\,520-536\,112r+4\,174\,761r^2-12\,734\,370r^3+18\,166\,056r^4\\
&-13\,785\,984r^5+5\,028\,608r^6)+8J_1^6J_2r(-108\,459+2\,561\,472r-17\,865\,060r^2+42\,056\,212r^3\\
&-43\,723\,408r^4+19\,466\,016r^5)+8J_1^5J_2^2r(-120\,123+3\,081\,636r-26\,591\,049r^2\\
&+104\,756\,322r^3-150\,488\,432r^4+82\,730\,944r^5)+4J_1^4J_2^3r(-205\,416+6\,235\,740r\\
&-66\,481\,989r^2+275\,607\,666r^3-543\,091\,408r^4+372\,472\,256r^5)+2J_1^3J_2^4r(-364\,932\\
&+10\,618\,461r-111\,258\,000r^2+530\,418\,656r^3-1\,116\,577\,664r^4+926\,078\,848r^5)\\
&+20J_1^2J_2^5r(-51\,678+1\,313\,703r-10\,031\,442r^2+34\,441\,608r^3-66\,122\,048r^4\\
&+61\,121\,472r^5)+80J_1J_2^6r(-4347+127\,044r-1\,130\,751r^2+3\,894\,570r^3-6\,116\,240r^4\\
&+4\,059\,904r^5)+3J_2^7(20\,520-536\,112r+4\,174\,761r^2-12\,734\,370r^3+18\,166\,056r^4\\
&-13\,785\,984r^5+5\,028\,608r^6)\big]
\end{aligned}
\tag{B1}
$$

and

$$
C(\beta) = Nk\sum_{n=2}^{\infty} d_n\beta^n
$$

$$
d_2 = \frac{2}{3}\big(J_1^2+J_2^2\big)r^2; \quad d_3 = \frac{1}{3}r^2\big(J_1^3-8J_1^2J_2r+J_2^3\big)
$$

$$
d_4 = \frac{2}{45}r^2\big[J_1^4(3-18r+7r^2)-20J_1^3J_2r+50J_1^2J_2^2r(-1+2r)+J_2^4(3-18r+7r^2)\big]
$$

$$
\begin{aligned}
d_5 = &\frac{1}{162}r^2\big[J_1^5(9-108r+28r^2)-8J_1^4J_2r(9-104r+16r^2)+40J_1^3J_2^2r(-3+5r)\\
&-4J_1^2J_2^3r(39-274r+256r^2)+J_2^5(9-108r+28r^2)\big]
\end{aligned}
$$

$$
\begin{aligned}
d_6 = &-\frac{1}{22\,680}r^2\big[J_1^6(-576+9756r-23\,739r^2+12\,160r^3+640r^4)+560J_1^5J_2r(9-135r+16r^2)\\
&-28J_1^4J_2^2r(-297+4023r-12904r^2+824r^3)+280J_1^3J_2^3r(24-153r+128r^2)\\
&-70J_1^2J_2^4r(-144+2139r-3872r^2+2400r^3)+J_2^6(-576+9756r-23\,739r^2+12\,160r^3+640r^4)\big]
\end{aligned}
$$

$$
\begin{aligned}
d_7 = &\frac{1}{97\,200}r^2\big[J_1^7(1242-25\,920r+116\,211r^2-58\,432r^3-1920r^4)+8J_1^6J_2r(-1503+28\,233r\\
&-99\,398r^2+31\,296r^3+3616r^4)+28J_1^5J_2^2r(-639+11\,076r-31\,508r^2+1648r^3)\\
&+56J_1^4J_2^3r(-279+5943r-42\,779r^2+59\,100r^3+64r^4)+42J_1^3J_2^4r(-306+4361r-7144r^2+4000r^3)\\
&-4J_1^2J_2^5r(5472-110\,007r+401\,658r^2-434\,720r^3+186\,560r^4)\\
&+J_2^7(1242-25\,920r+116\,211r^2-58\,432r^3-1920r^4)\big]
\end{aligned}
$$

$$
\begin{aligned}
d_8 = \frac{1}{1093\,500} r^2 \big[& J_1^8 (7695 - 185\,976r + 1\,160\,352r^2 - 1\,811\,898r^3 + 889\,724r^4 + 20\,256r^5 \\
& - 27\,512r^6) + 8J_1^7 J_2 r(-10\,044 + 212\,661r - 1\,119\,348r^2 + 371\,668r^3 + 27\,120r^4) \\
& - 2J_1^6 J_2^2 r(57\,672 - 1\,256\,355r + 7\,596\,708r^2 - 19\,368\,452r^3 + 3\,177\,376r^4 + 819\,808r^5) \\
& + 20J_1^5 J_2^3 r(-4536 + 111\,771r - 777\,870r^2 + 988\,176r^3 + 896r^4) - 2J_1^4 J_2^4 r(44\,874 \\
& - 1\,369\,062r + 13\,508\,715r^2 - 39\,201\,672r^3 + 31\,536\,928r^4 + 2\,049\,424r^5) - 20J_1^3 J_2^5 r(3618 \\
& - 69\,579r + 233\,613r^2 - 237\,744r^3 + 93\,280r^4) + 10J_1^2 J_2^6 r(-13\,662 + 325\,665r - 1\,954\,599r^2 \\
& + 3\,232\,376r^3 - 2\,405\,088r^4 + 818\,624r^5) + J_2^8 (7695 - 185\,976r + 1\,160\,352r^2 - 1\,811\,898r^3 \\
& + 889\,724r^4 + 20\,256r^5 - 27\,512r^6) \big].
\end{aligned} \tag{B2}
$$

Next we give the formulas for the asymmetric model (up to fifth order). For the susceptibility χ we find

$$
\chi(\beta) = N \sum_{n=1}^{\infty} c_n \beta^n;\ r = s(s+1)
$$

$$
c_1 = \frac{r}{3};\quad c_2 = -\frac{2}{9}(J_1' + J_1 + J_2' + J_2) r^2;
$$

$$
\begin{aligned}
c_3 = \frac{1}{54} r^2 \big\{ & -3\big(J_1'^2 + J_1^2 + J_2'^2 + J_2^2\big) + 4\big[J_1'^2 + J_1^2 + J_2'^2 + 4J_2' J_2 + J_2^2 + 4J_1(J_2' + J_2) + 4J_1'(J_1 + J_2' + J_2)\big] r \big\};
\end{aligned}
$$

$$
\begin{aligned}
c_4 = \frac{1}{405} r^2 \big\{ & -6\big(J_1'^3 + J_1^3 + J_2'^3 + J_2^3\big) + 3\big\{7J_1'^3 + 7J_1^3 + 10J_1^2(J_2' + J_2) \\
& + 10J_1'^2(J_1 + J_2' + J_2) + 10J_1\big(J_2'^2 + J_2^2\big) + (J_2' + J_2)\big(7J_2'^2 + 3J_2' J_2 + 7J_2^2\big) \\
& + 10J_1'\big[J_1^2 + J_2'^2 + J_2^2 + J_1(J_2' + J_2)\big]\big\} r - 4\big[J_1'^3 + J_1^3 + 20J_1^2(J_2' + J_2) \\
& + 20J_1'^2(J_1 + J_2' + J_2) + 20J_1\big(J_2'^2 + 3J_2' J_2 + J_2^2\big) + (J_2' + J_2)\big(J_2'^2 + 19J_2' J_2 + J_2^2\big) \\
& + 5J_1'\big[4J_1^2 + 9J_1(J_2' + J_2) + 4\big(J_2'^2 + 3J_2' J_2 + J_2^2\big)\big]\big] r^2 \big\};
\end{aligned}
$$

$$
\begin{aligned}
c_5 = \frac{1}{9720} r^2 \big\{ & -45\big(J_1^4 + J_2'^4 + J_2^4\big) + 192J_1'^3(J_1 + J_2' + J_2) r(1 - 6r + 4r^2) \\
& + 12J_1' r\big[16J_1^3 + 9J_1^2 J_2' + 9J_1 J_2'^2 + 16J_2'^3 + 9J_1^2 J_2 + 9J_1 J_2^2 + 16J_2^3 \\
& - 2\big(48J_1^3 + 87J_1^2(J_2' + J_2) + 12(J_2' + J_2)\big(4J_2'^2 + J_2' J_2 + 4J_2^2\big) + J_1\big(87J_2'^2 + 80J_2' J_2 + 87J_2^2\big)\big) r \\
& + 16(J_1 + J_2' + J_2)\big[4J_1^2 + 4J_2'^2 + 26J_2' J_2 + 4J_2^2 + 17J_1(J_2' + J_2)\big] r^2\big] \\
& - J_1'^4[45 + 4r(-69 + 4r(11 + r))] + 12J_1'^2 r\big\{30\big(J_2'^2 + J_2^2\big) - 80(J_2' + J_2)^2 r + 80(2J_2' + J_2)(J_2' + 2J_2) r^2 \\
& + 10J_1^2[3 + 8r(-1 + 2r)] + 3J_1(J_2' + J_2)[3 + 2r(-29 + 56r)]\big\} + 4r\big\{48J_2'^3 J_2(1 - 6r + 4r^2) \\
& + 48J_2' J_2^3(1 - 6r + 4r^2) + 48J_1^3(J_2' + J_2)(1 - 6r + 4r^2) + 30J_1^2\big[3\big(J_2'^2 + J_2^2\big) \\
& - 8(J_2' + J_2)^2 r + 8(2J_2' + J_2)(J_2' + 2J_2) r^2\big] + J_1^4[69 - 4r(11 + r)] \\
& + J_2'^4[69 - 4r(11 + r)] + J_2^4[69 - 4r(11 + r)] + 30J_2'^2 J_2^2[3 + 8r(-1 + 2r)] \\
& + 24J_1(J_2' + J_2)\big(2J_2'^2(1 - 6r + 4r^2) + 2J_2^2(1 - 6r + 4r^2) + J_2' J_2(-2 + r(-3 + 52r))\big)\big\}\big\}.
\end{aligned} \tag{B3}
$$

For the specific heat C we have

$$
C(\beta) = Nk \sum_{n=2}^{\infty} d_n \beta^n
$$

$$
d_2 = \frac{1}{3} r^2 \big(J_1'^2 + J_1^2 + J_2'^2 + J_2^2\big)
$$

$$
d_3 = \frac{1}{6} r^2 \big[J_1'^3 + J_1^3 + J_2'^3 + J_2^3 - 8J_1' J_1(J_2' + J_2) r\big]
$$

$$
\begin{aligned}
d_4 = \frac{1}{45} r^2 \big\{ & 3\big(J_1'^4 + J_1^4 + J_2'^4 + J_2^4\big) - 2\big[4J_1'^4 + 2\big(2J_1^4 + 5J_1^2 J_2'^2 + 2J_2'^4 + 5\big(J_1^2 + J_2'^2\big) J_2^2 + 2J_2^4\big) \\
& + 5J_1' J_1\big(J_2'^2 + J_2^2 + J_1(J_2' + J_2)\big) + 5J_1'^2\big(2J_1^2 + J_1(J_2' + J_2) + 2\big(J_2'^2 + J_2^2\big)\big)\big] r \\
& + \big[-3J_1'^4 - 3J_1^4 - 3J_2'^4 + 20J_2'^2 J_2^2 - 3J_2^4 + 20J_1^2\big(J_2'^2 + 3J_2' J_2 + J_2^2\big) + 20J_1'^2\big(J_1^2 + J_2'^2 + 3J_2' J_2 + J_2^2\big)\big] r^2 \big\}
\end{aligned}
$$

$$
\begin{aligned}
d_5 = \frac{1}{324} r^2 \{ & 9\left(J_1'^5 + J_1^5 + J_2'^5 + J_2^5\right) - 12\left[4J_1'^5 + 4J_1^5 + 5J_1^3\left(J_2'^2 + J_2^2\right) + (J_2' + J_2)\left(2J_2'^2 - J_2'J_2 + 2J_2^2\right)^2\right. \\
& + 5J_1^2\left(J_2'^3 + J_2^3\right) + 5J_1'^2\left(J_1^3 + J_2'^3 + J_2^3\right) + 3J_1'J_1\left(J_2'^3 + J_2^3 + J_1^2(J_2' + J_2)\right) \\
& \left. + J_1'^3\left(5J_1^2 + 3J_1(J_2' + J_2) + 5\left(J_2'^2 + J_2^2\right)\right)\right] r + 4\left[- 3J_1'^5 - 3J_1^5 - 3J_2'^5 + 10J_2'^3 J_2^2 + 10J_2'^2 J_2^3 - 3J_2^5\right. \\
& + 10J_1^3\left(J_2'^2 + 3J_2'J_2 + J_2^2\right) + 5J_1^2(J_2' + J_2)\left(2J_2'^2 + J_2'J_2 + 2J_2^2\right) + 8J_1'J_1(J_2' + J_2)\left(13\left(J_1^2 + J_2'^2\right)\right. \\
& \left. + 2J_2'J_2 + 13J_2^2\right) + 2J_1'^3\left(5J_1^2 + 52J_1(J_2' + J_2) + 5\left(J_2'^2 + 3J_2'J_2 + J_2^2\right)\right) \\
& \left. + 5J_1'^2\left(2J_1^3 + (J_2' + J_2)\left(2J_2'^2 + J_2'J_2 + 2J_2^2\right)\right)\right] r^2 - 64J_1'J_1(J_2' + J_2)\left(J_1'^2 + J_1^2 + J_2'^2 + 14J_2'J_2 + J_2^2\right) r^3 \}.
\end{aligned}
\tag{B4}
$$

APPENDIX C: THE HIGH-TEMPERATURE EXPANSION FOR THE SUSCEPTIBILITY AND THE SPECIFIC HEAT FOR THE HEISENBERG MODEL ON THE PYROCHLORE LATTICE

The general formulas for the susceptibility and the specific heat for the Heisenberg model on the pyrochlore lattice with NN exchange constant J up to eighth order read for the susceptibility as follows:

$$
\begin{aligned}
\chi(\beta) &= \frac{N}{J} \sum_{n=1}^{\infty} c_n (J\beta)^n \\
c_1 = \frac{r}{3}; \quad c_2 &= -\frac{2r^2}{3}; \quad c_3 = \frac{1}{18} r^2(-3 + 20r) \\
c_4 &= -\frac{1}{135} r^2(6 - 91r + 224r^2) \\
c_5 &= \frac{1}{1080} r^2(-15 + 376r - 1816r^2 + 2544r^3) \\
c_6 &= -\frac{1}{14\,175} r^2(72 - 2406r + 18\,909r^2 - 47\,188r^3 + 46\,848r^4) \\
c_7 &= \frac{1}{2\,041\,200} r^2(-4347 + 17\,6346r - 1\,901\,709r^2 + 7\,300\,134r^3 - 1\,1982\,944r^4 + 9\,482\,624r^5) \\
c_8 &= -\frac{1}{61\,236\,000} r^2(61\,560 - 2\,887\,056r + 38\,320\,749r^2 - 202\,461\,642r^3 + 477\,409\,712r^4 - 601\,876\,480r^5 + 399\,408\,640r^6)
\end{aligned}
\tag{C1}
$$

and for the specific heat

$$
\begin{aligned}
C(\beta) &= Nk \sum_{n=2}^{\infty} d_n (J\beta)^n \\
d_2 = r^2; \quad d_3 &= \frac{1}{6} r^2(3 - 8r); \quad d_4 = \frac{1}{15} r^2(3 - 38r + 7r^2) \\
d_5 &= \frac{1}{36} r^2(3 - 68r + 148r^2 + 32r^3) \\
d_6 &= -\frac{1}{45\,360} r^2(-1728 + 53\,964r - 301\,671r^2 + 102\,672r^3 + 56\,128r^4) \\
d_7 &= -\frac{1}{64\,800} r^2(-1242 + 47\,808r - 418\,437r^2 + 728\,520r^3 + 178\,240r^4 + 13\,312r^5) \\
d_8 &= \frac{1}{729\,000} r^2(7695 - 345\,816r + 3\,954\,204r^2 - 13\,638\,312r^3 + 5\,728\,812r^4 + 4\,024\,640r^5 + 1\,856\,680r^6).
\end{aligned}
\tag{C2}
$$

*Correspondence should be addressed to hschmidt@uos.de.

[1] M. Troyer and U. J. Wiese, Phys. Rev. Lett. **94**, 170201 (2005).

[2] U. Schollwöck, Rev. Mod. Phys. **77**, 259 (2005); Ann. Phys. (NY) **326**, 96 (2011).

[3] P. Froebrich and P. J. Kuntz, Phys. Rep. **432**, 223 (2006).

[4] D. Schmalfuß, J. Richter, and D. Ihle, Phys. Rev. B **72**, 224405 (2005).

[5] M. Härtel, J. Richter, D. Ihle, and S.-L. Drechsler, Phys. Rev. B **81**, 174421 (2010).

[6] G. S. Rushbrooke, G. A. Baker, and P. J. Wood, in *Phase Transitions and Critical Phenomena*, edited by C. Domb and M. S. Green (Academic Press, London, 1974), Vol. 3, p. 245.

[7] J. Oitmaa, C. J. Hamer, and W. H. Zheng, *Series Expansion Methods* (Cambridge University Press, Cambridge, UK, 2006).

[8] H.-J. Schmidt, J. Schnack, and M. Luban, Phys. Rev. B **64**, 224415 (2001).

[9] P. J. Wood and G. S. Rushbrooke, Proc. Phys. Soc. London A **70**, 765 (1957).

[10] K. Pirnie, P. J. Wood, and J. Eve, Mol. Phys. **11**, 551 (1966).

[11] C. A. Thuesen, H. Weihe, J. Bendix, S. Piligkos, and O. Monsted, Dalton Trans. **39**, 4882 (2010).

[12] P. J. Cregg, J. L. Garcia-Palacios, P. Svedlindh, and K. Murphy, J. Phys. Condens. Matter **20**, 204119 (2008).

[13] N. Fukushima, A. Honecker, S. Wessel, and W. Brenig, Phys. Rev. B **69**, 174430 (2004).

[14] J. Oitmaa and W. H. Zheng, Phys. Rev. B **69**, 064416 (2004).

[15] J. Oitmaa and W. H. Zheng, J. Phys. Condens. Matter **16**, 8653 (2004).

[16] M. Luban, P. Kögerler, L. L. Miller, and R. E. P. Winpenny, J. Appl. Phys. **93**, 7083 (2003).

[17] M. Shiroishi and M. Takahashi, Phys. Rev. Lett. **89**, 117201 (2002).

[18] A. Honecker and A. Lauchli, Phys. Rev. B **63**, 174407 (2001).

[19] A. Buhler, N. Elstner, and G. S. Uhrig, Eur. Phys. J. B **16**, 475 (2000).

[20] Weihong Zheng, C. J. Hamer, and J. Oitmaa, Phys. Rev. B **60**, 6608 (1999).

[21] N. Elstner and R. R. P. Singh, Phys. Rev. B **57**, 7740 (1998).

[22] N. Elstner and R. R. P. Singh, Phys. Rev. B **58**, 11484 (1998).

[23] J. Oitmaa and E. Bornilla, Phys. Rev. B **53**, 14228 (1996).

[24] J. Karwowski, D. BielinskaWaz, and J. Jurkowski, Int. J. Quantum Chem. **60**, 185 (1996).

[25] D. C. Johnston, R. K. Kremer, M. Troyer, X. Wang, A. Klümper, S. L. Bud'ko, A. F. Panchula, and P. C. Canfield, Phys. Rev. B **61**, 9558 (2000).

[26] H. Rosner, R. R. P. Singh, W. H. Zheng, J. Oitmaa, and W. E. Pickett, Phys. Rev. B **67**, 014416 (2003).

[27] G. Misguich, B. Bernu, and L. Pierre, Phys. Rev. B **68**, 113409 (2003).

[28] See Supplemental Material at http://link.aps.org/supplemental/10.1103/PhysRevB.84.104443 for a MATHEMATICA8.0.1 file containing a list of relevant graphs and the coefficients of the HTE of the moments, the magnetic moments, the free energy and the zero field susceptibility for general Heisenberg Hamiltonians up to eighth order.

[29] See Supplemental Material at http://link.aps.org/supplemental/10.1103/PhysRevB.84.104443 for a MATHEMATICA8.0.1 file containing the HTE coefficients up to eighth order for the susceptibility and the specific heat of the J_1-J_1'-J_2-J_2' model, cf. Eq. (41) and Fig. 5.

[30] [http://www.uni-magdeburg.de/jschulen/HTE/].

[31] G. A. Baker, Phys. Rev. **124**, 768 (1961).

[32] A. Müller, M. Luban, C. Schröder, R. Modler, P. Kögerler, M. Axenovich, J. Schnack, P. Canfield, S. Budko, and N. Harrison, ChemPhysChem **2**, 517 (2001).

[33] O. Waldmann, Coord. Chem. Rev. **249**, 2550 (2005).

[34] A. M. Todea, A. Merca, H. Bögge, J. Van Slageren, M. Dressel, L. Engelhardt, M. Luban, T. Glaser, M. Henry, and A. Müller, Angew. Chem. Int. Ed. **46**, 6106 (2007).

[35] A. M. Todea, A. Merca, H. Bögge, J. Van Slageren, M. Dressel, L. Engelhardt, M. Luban, T. Glaser, M. Henry, and A. Müller, Chem. Commun. **2009**, 3351 (2009).

[36] O. Waldmann, Phys. Rev. B **75**, 012415 (2007).

[37] C. Schröder, R. Prozorov, P. Kögerler, M. D. Vannette, X. Fang, M. Luban, A. Matsuo, K. Kindo, A. Müller, and A. M. Todea, Phys. Rev. B **77**, 224409 (2008).

[38] J. Schnack, H.-J. Schmidt, J. Richter, and J. Schulenburg, Eur. Phys. J. B **24**, 475 (2001); J. Richter, R. Schmidt, and J. Schnack, J. Magn. Magn. Mater. **295**, 164 (2005); I. Rousochatzakis, A. M. Läuchli, and F. Mila, Phys. Rev. B **77**, 094420 (2008).

[39] J. Schnack, M. Luban, and R. Modler, Europhys. Lett. **56**, 863 (2001); M. Exler and J. Schnack, Phys. Rev. B **67**, 094440 (2003).

[40] S. Torbrügge and J. Schnack, Phys. Rev. B **75**, 054403 (2007).

[41] J. Schnack, R. Schmidt, and J. Richter, Phys. Rev. B **76**, 054413 (2007).

[42] J. Schnack and O. Wendland, Eur. Phys. J. B **78**, 535 (2010).

[43] J. Schnack, e-print arXiv:1012.4980v1 (2010).

[44] P. Kögerler, B. Tsukerblat, and A. Mueller, Dalton Trans. **39**, 21 (2010).

[45] J. Schnack, Dalton Trans. **39**, 4677 (2010).

[46] J. Sirker, Zheng Weihong, O. P. Sushkov, and J. Oitmaa, Phys. Rev. B **73**, 184420 (2006).

[47] R. Darradi, O. Derzhko, R. Zinke, J. Schulenburg, S. E. Krüger, and J. Richter, Phys. Rev. B **78**, 214415 (2008).

[48] J. Reuther and P. Wölfle, Phys. Rev. B **81**, 144410 (2010).

[49] J. Richter and J. Schulenberg, Eur. Phys. J. B **73**, 117 (2010).

[50] J. Richter, R. Darradi, J. Schulenburg, D. J. J. Farnell, and H. Rosner, Phys. Rev. B **81**, 174429 (2010).

[51] G. Mendona, R. Lapa, J. R. de Sousa, M. A. Neto, K. Majumdar, and T. Datta, J. Stat. Mech. (2010) P06022.

[52] D. C. Johnston, R. J. McQueeney, B. Lake, A. Honecker, M. E. Zhitomirsky, R. Nath, Y. Furukawa, V. P. Antropov, and Y. Singh, e-print arXiv:1106.0206 (2011).

[53] A. A. Tsirlin and H. Rosner, Phys. Rev. B **79**, 214417 (2009).

[54] A. A. Tsirlin, R. Nath, A. M. Abakumov, R. V. Shpanchenko, C. Geibel, and H. Rosner, Phys. Rev. B **81**, 174424 (2010).

[55] R. Zinke, S.-L. Drechsler, and J. Richter, Phys. Rev. B **79**, 094425 (2009).

[56] O. Volkova *et al.*, Phys. Rev. B **82**, 054413 (2010).

[57] O. Janson, A. A. Tsirlin, and H. Rosner, Phys. Rev. B **82**, 184410 (2010).

[58] S. Nishimoto, S.-L. Drechsler, R. O. Kuzian, J. van den Brink, J. Richter, Y. Skourski, W. E. A. Lorenz, R. Klingeler, and B. Büchner, Phys. Rev. Lett. **107**, 097201 (2011).

[59] J.-K. Kim and M. Troyer, Phys. Rev. Lett. **80**, 2705 (1998).

[60] K. Harada, M. Troyer, and N. Kawashima, J. Phys. Soc. Jpn. **67**, 1130 (1998).

[61] N. Shannon, B. Schmidt, K. Penc, and P. Thalmeier, Eur. Phys. J. B **38**, 599 (2004).

[62] B. Schmidt, N. Shannon, and P. Thalmeier, J. Phys. Condens. Matter **19**, 145211 (2007).

[63] B. Schmidt, N. Shannon, and P. Thalmeier, J. Magn. Magn. Mater. **310**, 1231 (2007).

[64] R. Moessner, Can. J. Phys. **79**, 1283 (2001).

[65] S. T. Bramwell and M. J. P. Gingras, Science **294**, 1495 (2001).

[66] C. Castelnovo, R. Moessner, and S. L. Sondhi, Nature **451**, 42 (2008).

[67] J. N. Reimers, Phys. Rev. B **45**, 7287 (1992).

[68] R. Moessner and A. J. Berlinsky, Phys. Rev. Lett. **83**, 3293 (1999).

[69] A. J. Garcia-Adeva and D. L. Huber, Phys. Rev. B **63**, 140404 (2001).